CHAPTER IV

RESULTS AND DISCUSSION

In this research, the results obtained from all experiments were separated into four issues due to their characteristics which were the addition of acetyl acetone, the calcination temperature, the number of coating cycles and the appropriate wavelengths. Titanium (IV) butoxide was used as a precursor, ethanol used as a solvent, HCl used as an acidic catalyst and acetyl acetone used as an additive in terms of the mole ratio of Ti (IV) butoxide : ethanol : HCl : acetyl acetone at 1 : 30 : 0.5 : 1, respectively (Pongpom, 2004). A dimension of the prototype fixed bed photocatalytic reactor (FBPR) which was used to find the optimum conditions of TiO_2 thin films derived from the sol-gel pathway as shown in Table 4.1.

The fixed bed photocatalytic reactor (FBPR) is made from aluminums because the aluminum gives the best reflection of the UV light and also the dimension which is dependable upon other available equipment, i.e. the length of the UV lamps, the height of wastewater, and the flow rate of a pump. So, Table 4.1 showed the dimension of the fixed bed photoreactor which was used in all experiments in this work.

Table 4.1 The dimension of the fixed bed photocatalytic reactor (FBPR)

Length of reactor (cm.)	66.00
Width of reactor (cm.)	33.00
Height of reactor (cm.)	12.00
Length of plates (cm.)	10.80
Width of plates (cm.)	10.60
Thickness of plates (cm.)	0.1
Number of plates	18
Total thin film coating area of plates (cm^2)	$\approx$1980

For the TiO$_2$ thin film preparation, the characteristics of TiO$_2$ thin films on stainless steel plates using the sol-gel technique were investigated under four parameters. Four studied parameters were the addition of acetyl acetone, the number of coating cycles, the calcination temperatures and the appropriate wavelengths. All parameters were tested underlying the same controlled operating conditions as shown in Table 4.2.

Table 4.2 The operating conditions which were used to examine all studied parameters

Operating conditions	Value
Flow rate (ml/s)	80
Height of the wastewater (cm)	4
The number of plates	18
Total TiO$_2$ coating area (cm^2)	1,980

4.1 Effect of acetyl acetone addition

In this test, the characteristics of TiO$_2$ thin films which were prepared in mole ratio of Ti (IV) butoxide : ethanol : HCl : acetyl acetone at 1 : 30 : 0.5 : 1, respectively (Pongpom, 2004) and calcined at 500 °C in a furnace for 30 minutes with and without acetyl acetone with three coating cycles were indicated bellow:

4.1.1 The physical properties

4.1.1.1 Adhesive test

The adhesive test (ASTM D3359-95a) was supplied by the adhesive tape (the scotch tape) to examine the stability, uniformity and adherence of the TiO$_2$ thin layers. Table 4.3 showed the results of the TiO$_2$ thin films prepared with and without the adding of acetyl acetone were passed this test.

Table 4.3 The results of the TiO₂ thin films prepared with and without
the adding of acetyl acetone

Conditions	Testing
TiO₂ thin films derived with acetyl acetone	passed
TiO₂ thin films derived without acetyl acetone	passed

4.1.1.2 Corrosive test

From the results of this acid-alkali test, all of the prepared conditions were passed the test. This test was applied to find the film robustness and corrosive resistance under the acidic and basic conditions, which were HNO_3 and NaOH representing the strong acid and strong base, respectively. The results were shown in Table 4.4.

Table 4.4 The results of the TiO₂ thin films prepared with and without
the adding of acetyl acetone

Acidic and Basic conditions	TiO₂ with acetyl acetone	TiO₂ without acetyl acetone
1 M HNO_3	p	p
5 M HNO_3	p	p
10 M HNO_3	p	p
1 M NaOH	p	p
5 M NaOH	p	p
10 M NaOH	p	p

P = passed

4.1.2 Crystallization of TiO_2 thin films by XRD (X-ray diffraction)

From XRD analysis, the TiO_2 thin films are glazed on stainless steel plates with three coating cycles which is suitable for detecting the intensity of the anatase peak. Figure 4.1 illustrated the X-ray diffraction patterns of TiO_2 thin films with and without acetyl acetone used as an additive. It is shown that the majority of the anatase peak is at the angle of 25.28°, however, the minority of the anatase peak is representing at the angle of 36.94°, 37.8° and 38.58°. The different mole ratio of TiO_2 with and without acetyl acetone would affect the photocatalytic activities. Additionally, the difference of both conditions is the color of the sol-solution. A TiO_2 solution with acetyl acetone is yellow and transparent, but a TiO_2 solution without acetyl acetone is colorless and transparent.

From the crystalline patterns, it is found that the intensity of the anatase peak is not significantly different. The TiO_2 solution with acetyl acetone gives a little higher intensity of the anatase phase than the TiO_2 solution without acetyl acetone. Regarding to the calcination temperature at 500 °C, the rutile phase disappeared because the heat-treatment of TiO_2 controlled the amorphous to the anatase phase as the temperature increased from 400-900 °C. When the TiO_2 thin films were annealed over 1100 °C, the intensity of the rutile peak greatly increased while the anatase peak nearly disappeared (Kim et al., 2001).

The crystallite size of the anatase phase can be determined by the Debye-Scherrer equation (Horikoshi et al., 2001; Roquerol et al., 1998) from the main anatase peak represents at the angle of 25.28 °. The crystallite sizes of the TiO_2 thin films with and without acetyl acetone are shown in Table 4.5. It is important to note that the TiO_2 thin films with acetyl acetone make the smaller anatase structure than the TiO_2 thin films without acetyl acetone as indicated in Table 4.5. However, acetyl acetone plays an important role as a stabilizing agent to help the crystalline structure getting smaller and accelerate the photacatalytic process.

Table 4.5 Crystallite size of TiO_2 thin films derived from the TiO_2 solution with and without acetyl acetone

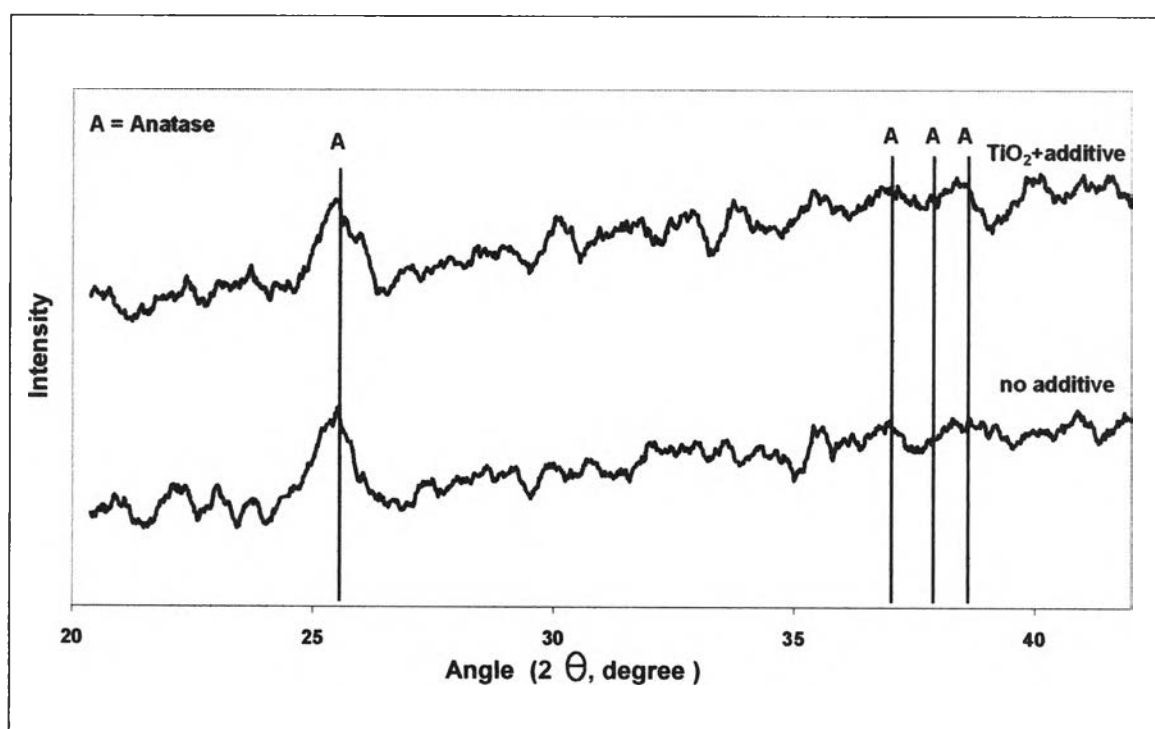| Mole ratio of Ti(IV) butoxide : ethanol : HCl : acetyl acetone	Crystalline size (nm)
1 : 30 : 0.5 : 1 (with acetyl acetone)	16.30
1 : 30 : 0.5 : 0 (without acetyl acetone)	20.38

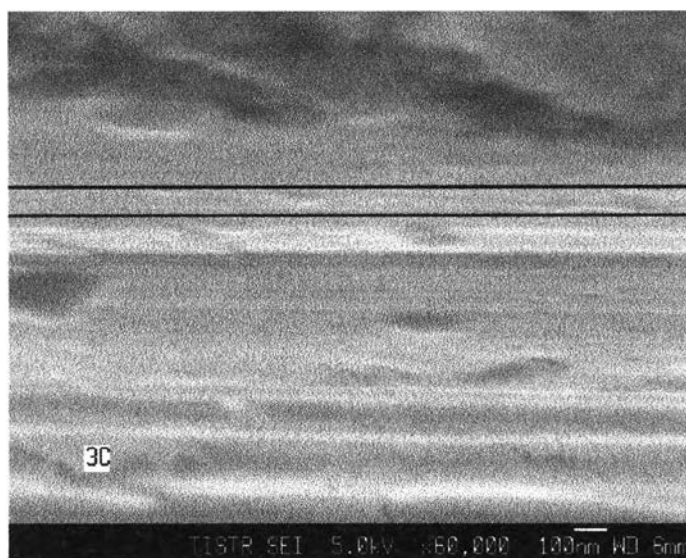**Figure 4.1** XRD patterns of TiO_2 thin films derived from the TiO_2 solution with and without acetyl acetone

4.1.3 Thickness

In this study, the thickness of all TiO_2 thin films conditions was estimated by a field-emission scanning electron microscopy (FE-SEM, JEOL model JSM-634 OF). It is interesting to note that the thickness of the TiO_2 thin films derived with acetyl acetone used as an additive would be less than the TiO_2 thin films prepared without acetyl acetone as seen in Table 4.6. This can be assumed that when acetyl acetone is added into the TiO_2 solution, the crystalline structures become smaller than another solution. It is connected to the experiment of the photocatalytic activities in the next section. Besides, the nanocrystalline thin layer thickness were photographed as illustrated in Figure 4.2

Table 4.6 The thickness of the TiO_2 thin films prepared with and without acetyl acetone

TiO_2 conditions	Thickness (nm)
with acetyl acetone	91
without acetyl acetone	117

60,000 magnifications

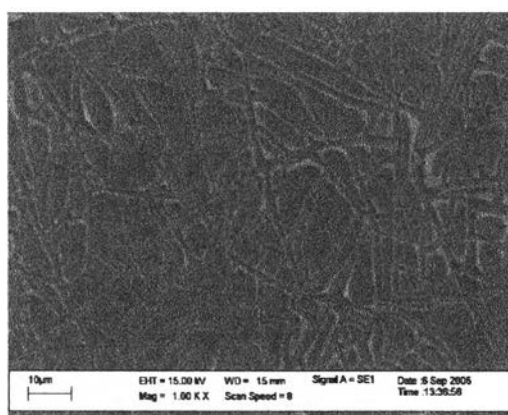(a) TiO_2 thin films prepared with acetyl acetone
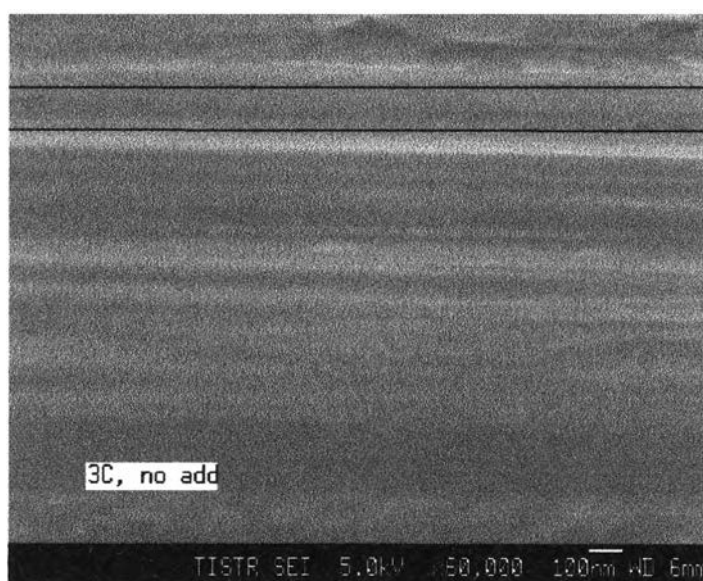
60,000 magnifications

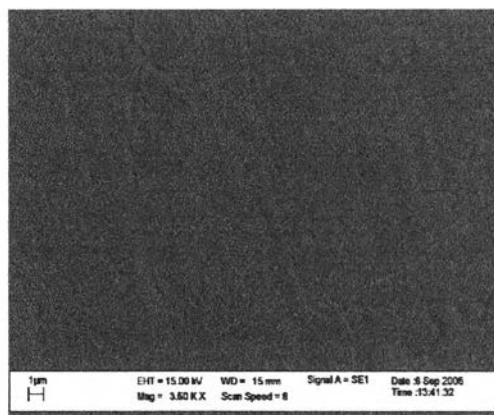(b) TiO_2 thin films prepared without acetyl acetone

Figure 4.2 (a) and (b) FE-SEM photographs of TiO_2 thin films derived from the TiO_2 sol-solutions with and without acetyl acetone

### 4.1.4 The morphology of TiO₂ with and without acetyl acetone

SEM (Scanning electron microscope) is a technique that is widely used for photographing the surface morphology. Figure 4.3 (a) and (b) demonstrated the surface morphology of the TiO_2 sheet derived from TiO_2 solutions with and without acetyl acetone. When applying acetyl acetone into the sol-solution, the surface morphology is better and smoother. The fracture of the films formed with acetyl acetone is less than a sheet formed without acetyl acetone. In this experimental case, the presence of acetyl acetone in the sol-solution would give more stable and consistent.
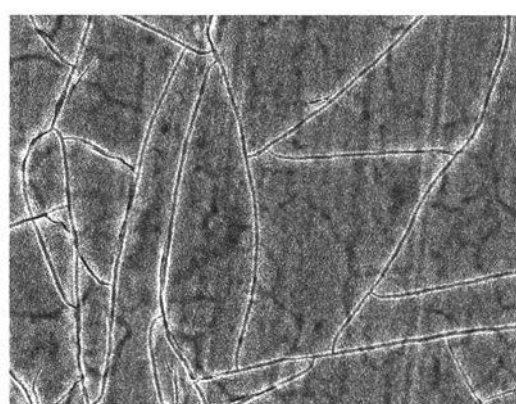

| 1000x magnification | 3500x   magnification |

(a) TiO_2 thin films prepared with acetyl acetone
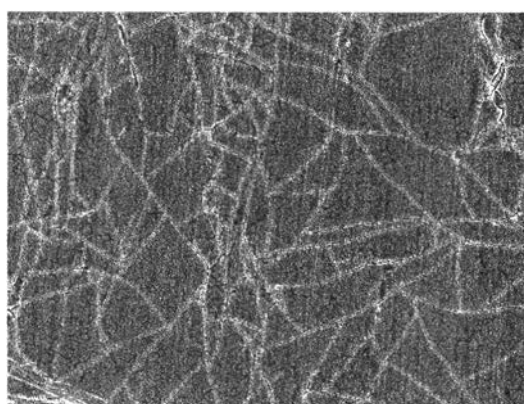
| 1000x magnification | 3500x   magnification |

(b) TiO_2 thin films prepared without acetyl acetone

Figure 4.3   (a) and (b) SEM photographs of TiO_2 thin films derived from the TiO_2 sol-solutions with and without acetyl acetone

In conclusion, the efficiency can be determined by all information of the results of all characteristics. For example, the XRD patterns, the crystalline size, the thickness, and the SEM micrographs of the TiO_2 thin films derived from the TiO_2 sol-solutions with acetyl acetone that are noticed corresponding to the smaller crystallite will make the smaller thickness and as shown in the SEM micrographs, the surface morphology is smoother than another condition.

4.1.5 Kinetic coefficient of the photocatalytic reduction

To compare the photocatalytic activity, the efficiency and the kinetic coefficient value (k) of hexavalent chromium in synthetic wastewater removal are judged by the zero order kinetic equation. The photocatalytic reduction reactions occur with respect to the initial concentration could be elucidated as the reaction with an apparent equation:

$$\frac{d[C]}{dt} = -k[C]^n$$

Where;   k   =   the apparent kinetic coefficient,

n   =   the reaction order (this case is zero order, so n = 0)

As shown in Figure 4.4, both reactions are the zero order reactions. So, the rate constant can be attained from this equation as follows:

$$\frac{d[C]}{dt} = -k[C]^n$$

Where n = 0; $[C]^n = 1$

$$\int_{C_o}^{C_t} d[C] = \int_0^t -kdt$$

$$C_t - C_o \quad = \quad -kt$$

$$\mathbf{C_t} \quad = \quad \mathbf{-kt + C_o}$$

The kinetic coefficient value (k) is increased with the adding of acetyl acetone. This phenomenon is in agreement with the increasing of the reaction rate of the photocatalytic reduction.

The photocatalytic reduction activities of the TiO_2 thin films using the TiO_2 sol-solution with and without acetyl acetone were shown in Figure 4.4. It is seen that the TiO_2 thin films with acetyl acetone make the reaction rate faster than the TiO_2 thin films without acetyl acetone.

Not only the reaction rates, but also the kinetic coefficient values (k) are different and tend to be increased corresponding to the addition of acetyl acetone. Figure 4.4 indicated the reactions at which made the different kinetic coefficients. Table 4.7 showed the kinetic coefficient (k).
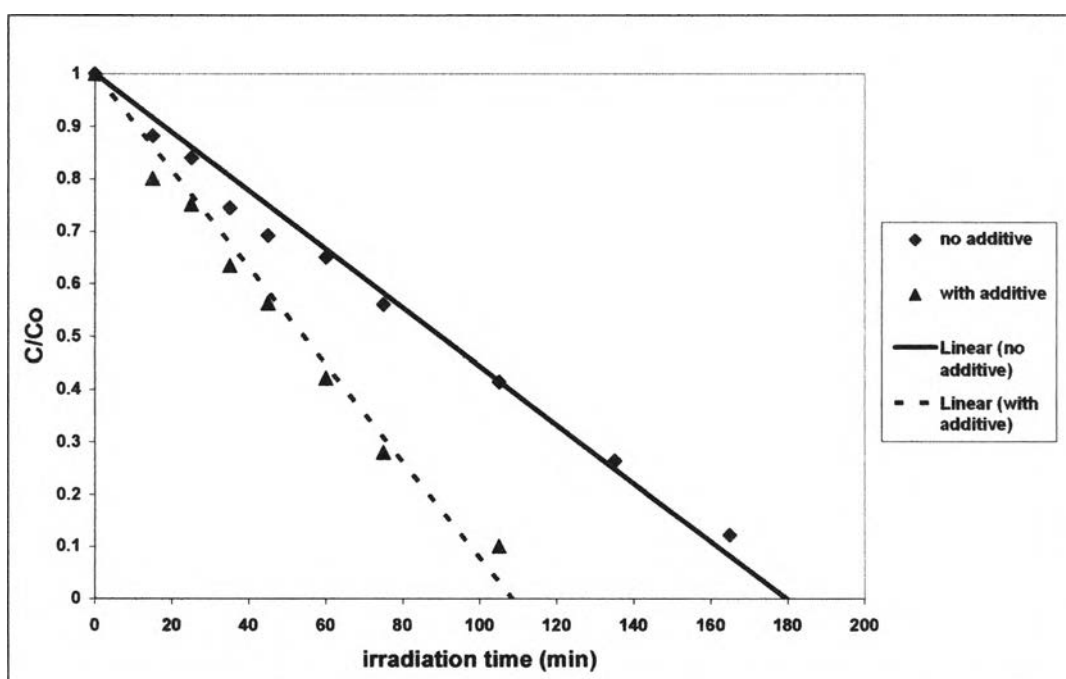

Figure 4.4   The photocatalytic reduction of Cr (VI) removal on the TiO_2

thin films derived from the solution with and without acetyl acetone

Table 4.7 The kinetic coefficient values of the TiO_2 thin films derived from the solution with and without acetyl acetone

Condition	TiO_2 with acetyl acetone	TiO_2 without acetyl acetone
Kinetic coefficient (k, mg/L* min)	0.2306	0.1391
R^2	0.9793	0.9841

In this case, acetyl acetone comes into play as a stabilizing agent in the acidic condition due to HCl (hydrochloric acid). The underlying reduction reaction mechanism is basically imitations of natural photolysis according to the photocatalytic reduction. Interestingly, the addition of acetyl acetone would produce the smaller particles that could provide the larger surface area of TiO_2. So, the higher surface area of TiO_2 gives the higher efficiency for Cr (VI) removal which can be indicated corresponding to the kinetic coefficient values (k).

From the different conditions of TiO_2 thin films, the time to complete the reaction is also different. It is noted that the TiO_2 thin films prepared with acetyl acetone would spend less time than the TiO_2 thin films prepared without acetyl acetone. Table 4.8 manifested the time to complete both reactions.

Table 4.8 The time to complete both reactions (irradiation time, min)

Condition	Time to complete the reaction (min)
TiO_2 thin films prepared with acetyl acetone	109
TiO_2 thin films prepared without acetyl acetone	179

From the above information, it is found that acetyl acetone will affect the efficiency of the photocatalytic reduction due to its property as a stabilizing agent to produce the smoother and thinner film. However, acetyl acetone does not cause the intensity of the anatase phase as found in Figure 4.1 (the XRD patterns). It is seen that the intensity of the anatase structure is still the same.

Besides, the kinetic coefficient (k) of the TiO_2 derived with acetyl acetone in the photocatalysis would be higher than another. So, the reasons that help the reaction rates move faster and make good conditions are acetyl acetone may help the surface morphology of TiO_2 be smoother. In addition, acetyl acetone produces the small particle size of TiO_2 that can easily increase the surface active sites as shown the nanocrystalline size in Table 4.5. Consequently, the TiO_2 thin films obtained from the TiO_2 sol-solution in the presence of Acetyl acetone in the ratio of Ti (IV) butoxide : ethanol : HCl : acetyl acetone equal to 1 : 30 : 0.5 : 1 was taken to study the effect of the calcination temperatures.

4.2 Effect of the calcination temperatures

The best condition of TiO_2 containing the previous ratio (Ti (IV) butoxide : ethanol : HCl : acetyl acetone equal to 1 : 30 : 0.5 : 1, respectively) was used to find the effect of the calcination temperatures. After the dip-coating process, the TiO_2 gel with three coating layers were heated at the range temperature from 300-500 °C in an electric furnace for 30 minutes.

4.2.1 The physical properties

4.2.1.1 Adhesive test

The adhesive test (ASTM D3359-95a) was supplied by the adhesive tape (the scotch tape) to examine the stability, uniformity and adherence of the TiO_2 thin layers.

Table 4.9 showed the results of the TiO_2 thin films calcined at different temperatures were passed this test.

Table 4.9 The results of TiO_2 thin layers which were prepared with the different calcination temperatures

The different calcination temperatures (°C)	Testing
300	passed
400	passed
450	passed
500	passed

4.2.1.2 Corrosive test

From the results of this test, all of the prepared conditions were passed the test. This test was applied to find the film robustness and corrosive resistance under the acidic and basic conditions. The results were shown in Table 4.10.

Table 4.10 The results of TiO_2 thin layers which were prepared with the different calcination temperatures

Acidic and Basic conditions	300 °C	400 °C	450 °C	500 °C
1 M HNO_3	p	p	p	p
5 M HNO_3	p	p	p	p
10 M HNO_3	p	p	p	p
1 M NaOH	p	p	p	p
5 M NaOH	p	p	p	p
10 M NaOH	p	p	p	p

P = passed

4.2.2 Crystallization of TiO₂ thin films by XRD (X-ray diffraction)

The attainable condition from the earlier test was defined the crystallite size by XRD technique. Figure 4.5 showed the XRD conformation of the TiO₂ films provided from the sol-gel process with the different heat-treatment.

It might be found that the intensity of the anatase phase is the highest; of course, the calcination temperature at 500 °C produces the highest yield. The crystallite size tends to be decreased with the increasing temperatures. Pongpom, 2004 found that at over 500 °C, the anatase crystal structure would transform to the rutile phase even at 600 °C. Below 400 °C no peaks of anatase showed, when the heat-treatment temperature was over 450 °C, TiO₂ films showed obvious peaks of anatase (Yu et al., 2000). According to the previous study (Hu et al., 1992), it was noted that the TiO₂ films obtained at lower 400 °C were amorphous. Because of the lack of the heat-resistance of stainless steel plates, the heating temperature more than 500 °C was not attainable.

In this case, the highest calcination temperature was at 500 °C. If the heat-treated over 500 °C, the structure of material would change the form and become FeO (Ferrous oxide) on the top of the surface area (Amornchat, 2004). The dissimilarity of this conversion might correlate the crystalline structure and size of TiO₂ films (Amornchat, 2004) as shown in Table 4.11. Figure 4.6 implied the trend of the crystallite size and the calcination temperatures which tended to be decreasing with an increasing heat-treatment. It is seen that the calcination temperatures would affect the crystalline size directly. So, this is the main result for the effect of the calcination temperatures.

Table 4.11 Crystallite sizes of TiO_2 films prepared from varied calcination temperature

The varied calcination tempetures (°C)	Crystalline size (nm)
300	0
400	23.54
450	20.60
500	16.3
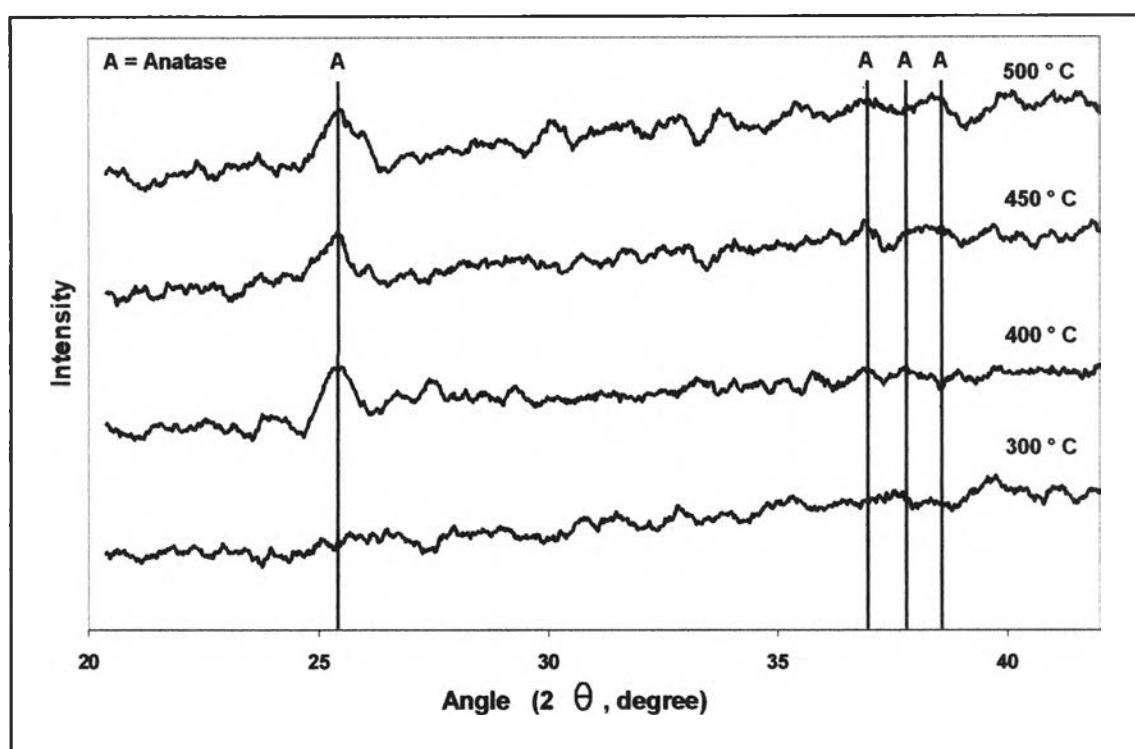
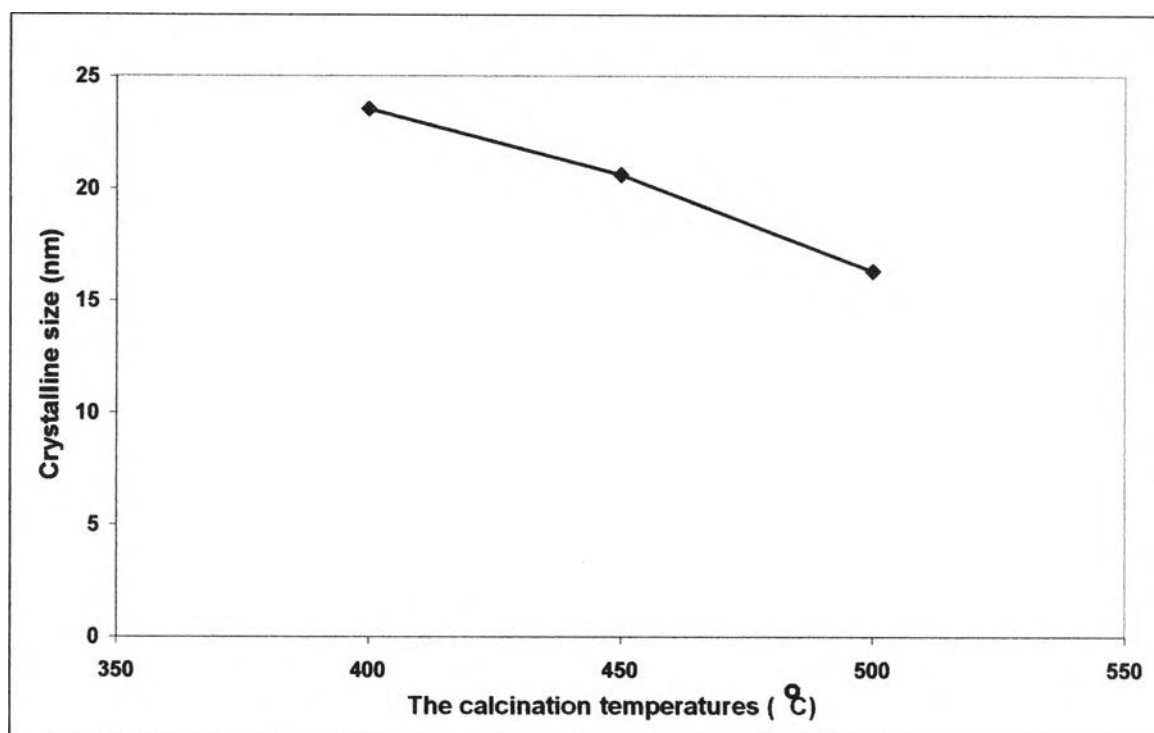**Figure 4.5** XRD patterns of TiO_2 thin films derived from the different calcination temperature

Figure 4.6 The plot of the crystallite size and the calcination temperatures

This is to say that when the heat-treated temperatures have been increasing, the crystalline sizes of TiO_2 would be decreased according to the form of the TiO_2 structure becomes the anatase structure as depicted in Figure 4.6.

4.2.3 Thickness

It has been seen that the thickness of the TiO_2 thin films prepared with different calcination temperatures is not different. At the three coating cycles, the thickness has the same size. The thickness of TiO_2 with three coating cycles calcined at different temperatures is approximately 100 nm as revealed in Table 4.12. Figure 4.7 implied the plot of the thickness versus the calcination temperatures. It is easy to describe that the trend is still remain the same.

Table 4.12   The thickness of the TiO$_2$ thin films prepared with
different calcination temeratures

The varied calcination tempetures (°C)	Thickness (nm)
300	103
400	100
450	104
500	91
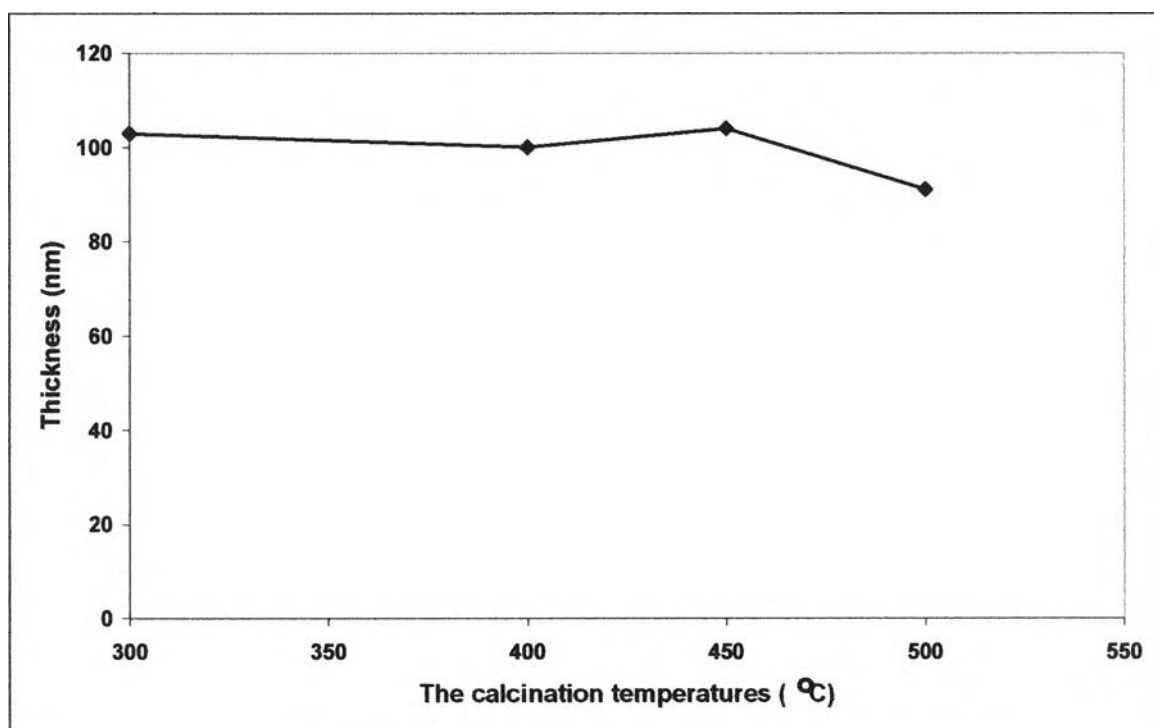
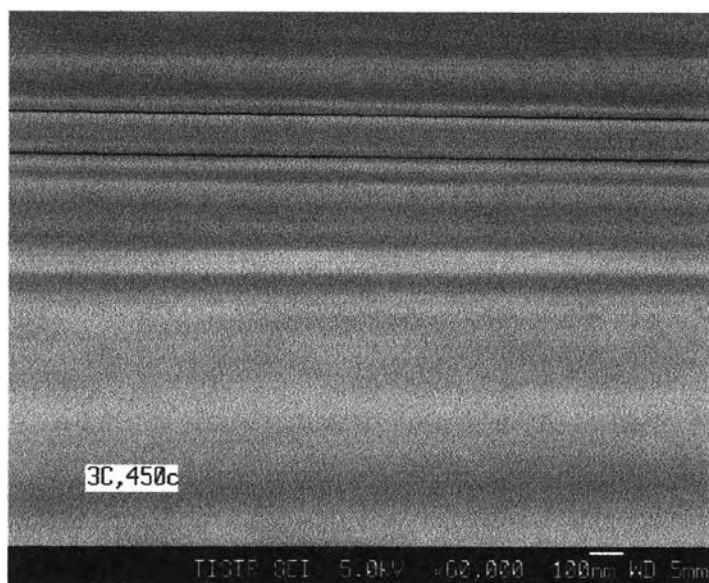**Figure 4.7**   The plot of the thickness VS the calcination temperatures
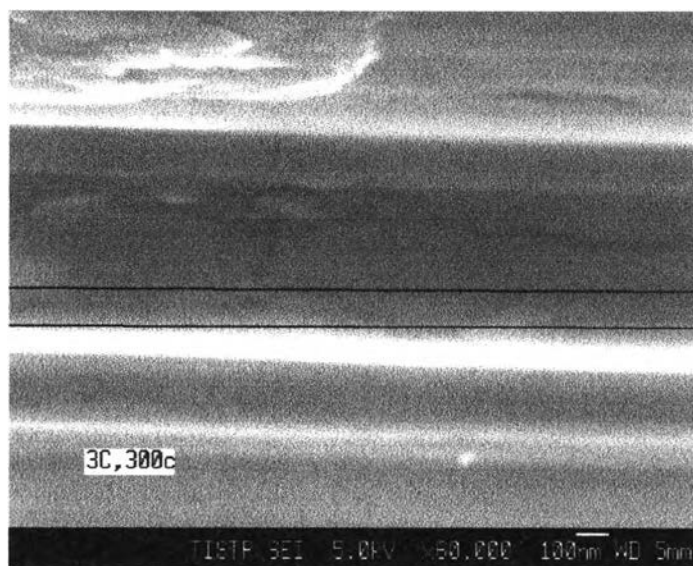
60,000 magnifications
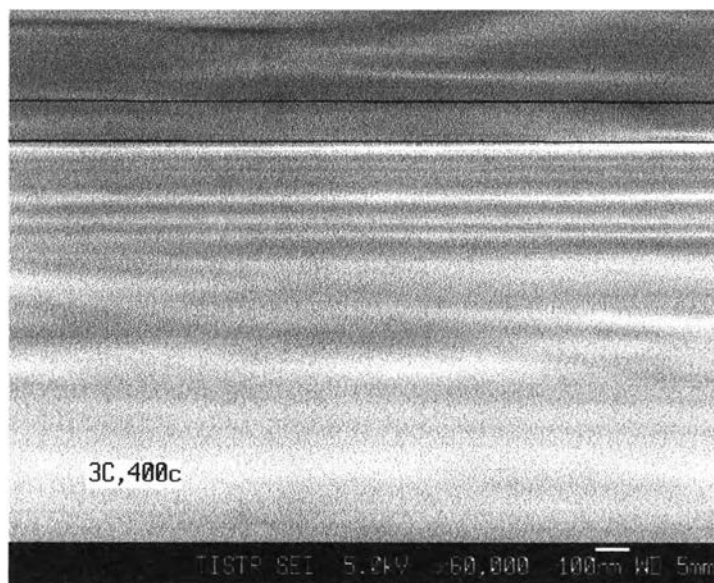
(a) TiO_2 thin films calcined at 300 °C

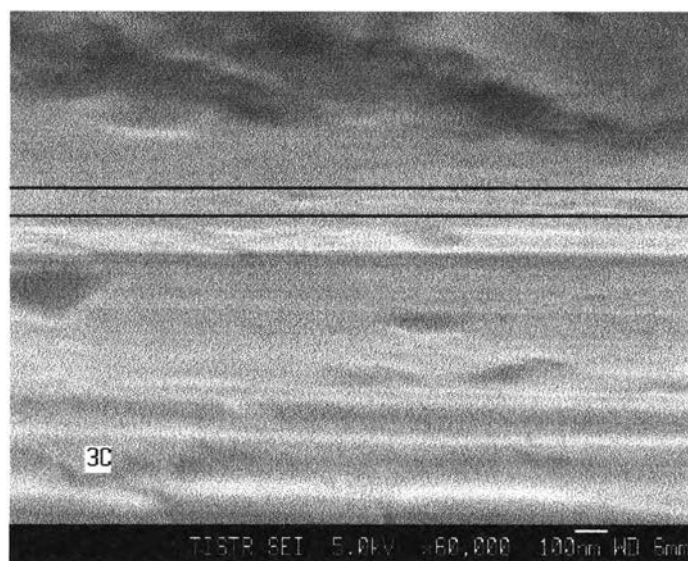60,000 magnifications
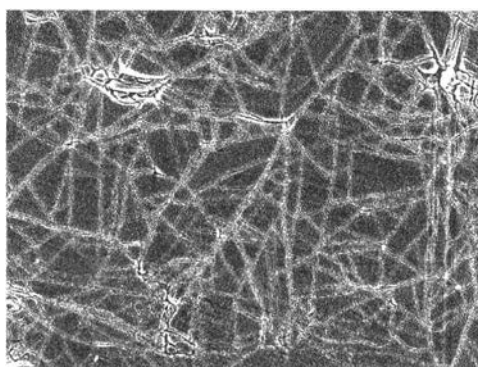
(b) TiO_2 thin films calcined at 400 °C

3C,450c

TISTR SEI 5.0kV ×60,000 100nm WD 5mm

60,000 magnifications

(c)   TiO$_2$ thin films calcined at 450 °C

3C

TISTR SEI 5.0kV ×60,000 100nm WD 6mm

60,000 magnifications

(d)   TiO$_2$ thin films calcined at 500 °C

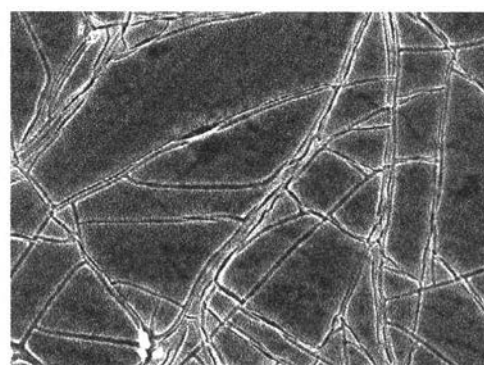**Figure 4.8**   FE-SEM micrographs of TiO$_2$ thin films calcined
at the various temperatures

Figure 4.8 showed the FE-SEM micrographs of TiO_2 thin films calcined at the various temperatures with 60,000 magnifications. The gap is the thickness representing in that condition.

4.2.4 The morphology of TiO_2 annealed at the various temperatures

SEM micrographs of TiO_2 thin films calcined at different temperatures were shown in Figure 4.9. In order to Figure 4.9, (a) – (d) show the fractures of TiO_2 thin films varying temperatures from 300-500 °C. All fabricated films are found to be uniform. It is clearly seen that mostly cracks occur at the low temperature; for example at 300 °C and 400 °C. Most of these thin layers are amorphous but small crystals of anatase can also exist (Lottiaux et al., 1989). Actually, the morphology of TiO_2 thin films at 500 °C is the smoothest and no cracks appear. According to the previous study (Negishi et al., 1995), the anatase to rutile phase transformation took place at temperatures of 600-800 °C. Even though, the phase transformation occurred at 1000 °C (Kim et al., 2001). In conclusion, TiO_2 thin films calcined at 500 °C is the best condition to remove chromium (VI) in pollutants. It was reported that the density of the TiO_2 increased with increasing the flaming temperature and with the heating rate in the framing process, resulting in higher refractive index (Keddie et al., 1990).
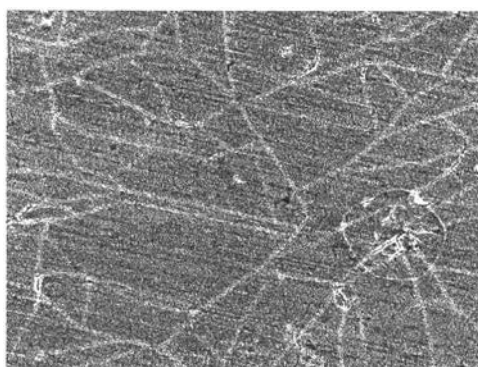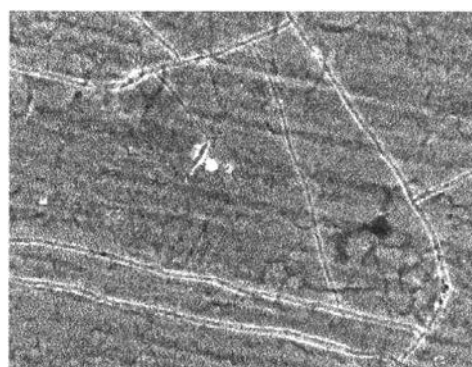

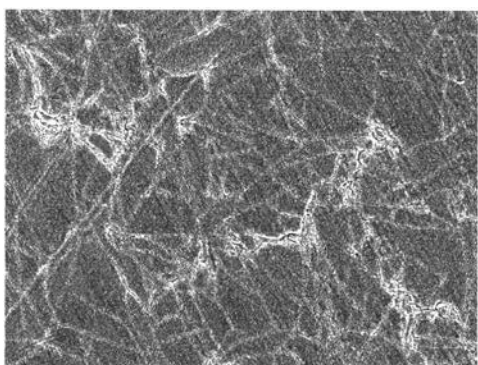| 1000x magnification | 3500x magnification |

(a) TiO_2 thin films calcined at 300 °C
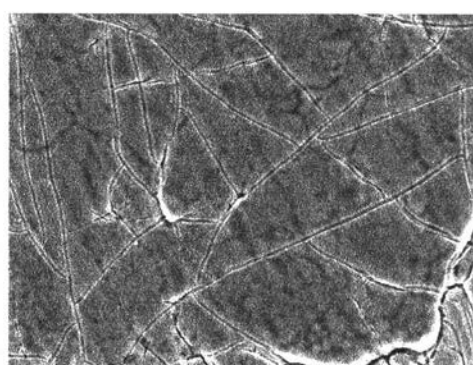
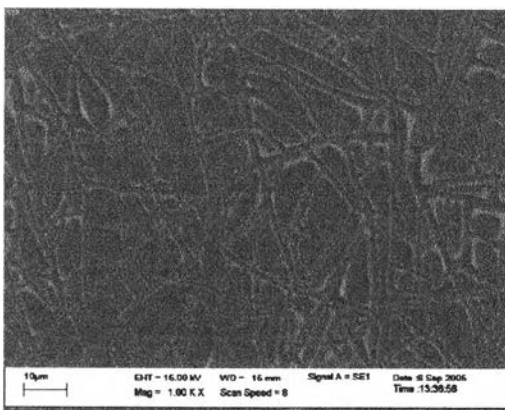1000x magnification   3500x magnification

(b)   TiO$_2$ thin films calcined at 400 °C

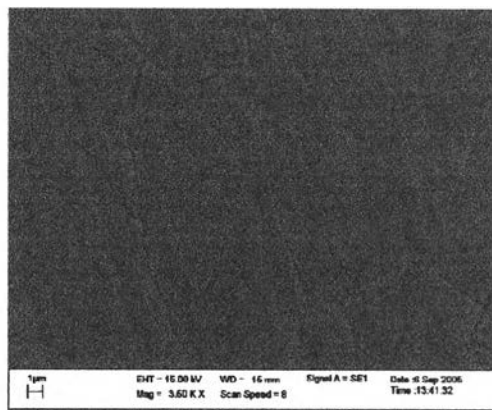1000x magnification   3500x magnification

(c)   TiO$_2$ thin films calcined at 450 °C

1000x magnification   3500x magnification

(d)   TiO$_2$ thin films calcined at 500 °C

Figure 4.9   SEM micrographs of TiO$_2$ thin films calcined at various temperatures

4.2.5 Kinetic coefficient of the photocatalytic reduction

The photocatalytic activities of TiO_2 thin films annealed at the various temperatures were shown in Figure 4.10. The kinetic coefficient (k) values increase with the expanding heat-treatment from 300 °C to 500 °C. Correspondingly, the TiO_2 thin films annealed at 500 °C make the highest efficiency on photocatalytic process. Table 4.13 illustrated the kinetic coefficient values due to the various temperatures. The gaining information from this phenomenon is the kinetic coefficient value (k) would be increased with the increasing the anatase phase due to the various temperatures. Especially, this calcination temperature at 500 °C was used to investigate the effect of the number of coating cycles in the next experiment.
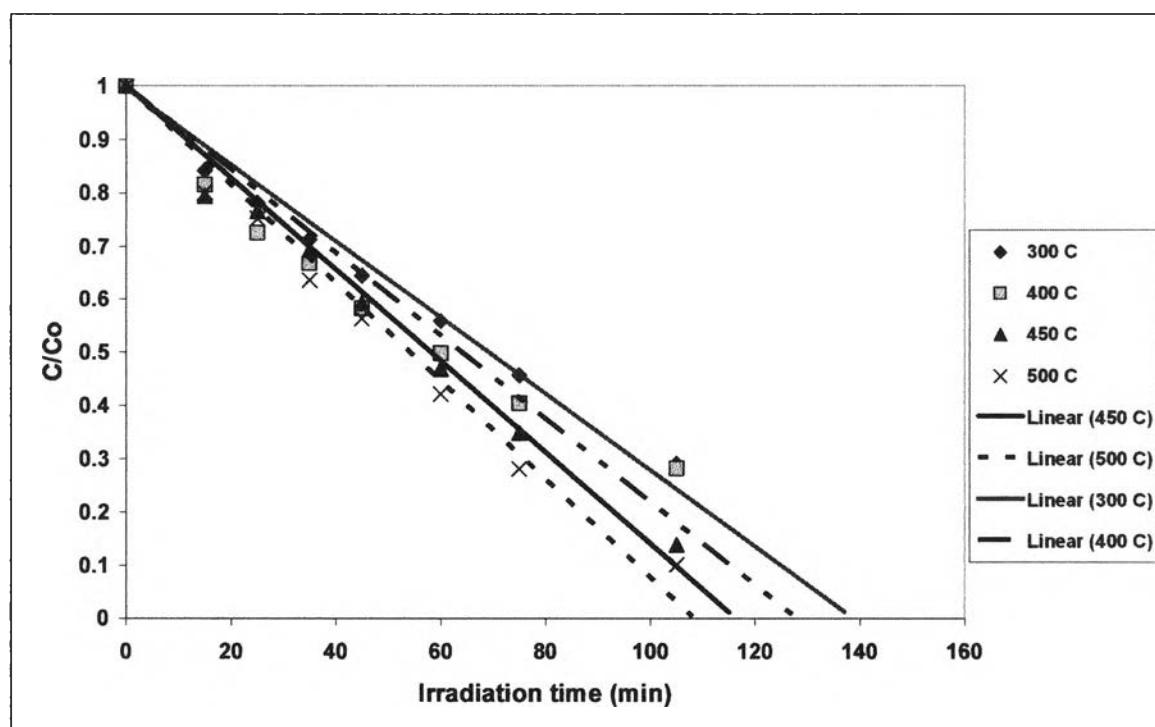

Figure 4.10   The photocatalytic reduction of Cr (VI) removal on the TiO_2 thin films derived at the various temperatures

Table 4.13 The kinetic coefficient values of the TiO_2 thin films
derived at the various temperatures

Calcination temperatures (°C)	Kinetic coefficient (k) (mg/L*min)	R^2
300	0.1805	0.976
400	0.1953	0.9183
450	0.2149	0.9835
500	0.2306	0.9793

It is ultimately seen that at 500°C, k is the highest but it has the lowest thickness and also the crystalline size is the lowest representing at this temperature.

According to the kinetic coefficient value (k), the plot of k VS the calcination temperature was shown in Figure 4.11. It can be found that the trend increases with the increasing temperatures. The reaction moves very fast depending on the anatase phase annealed at the optimum temperature (500 °C). In addtion k values will be varied by the temperatures. When the temperatures increase, the amorphous would be changed to the anatase structure of TiO_2 which the size is smaller than the amorphous. So, the particle size of TiO_2 will be smaller, that can give the larger active surface area of TiO_2. Thus, the more active surface area, the more efficiency of photocatalytic reduction occurs. Besides, the more efficiency of photocatalytic reduction, the more kinetic coefficient presents.
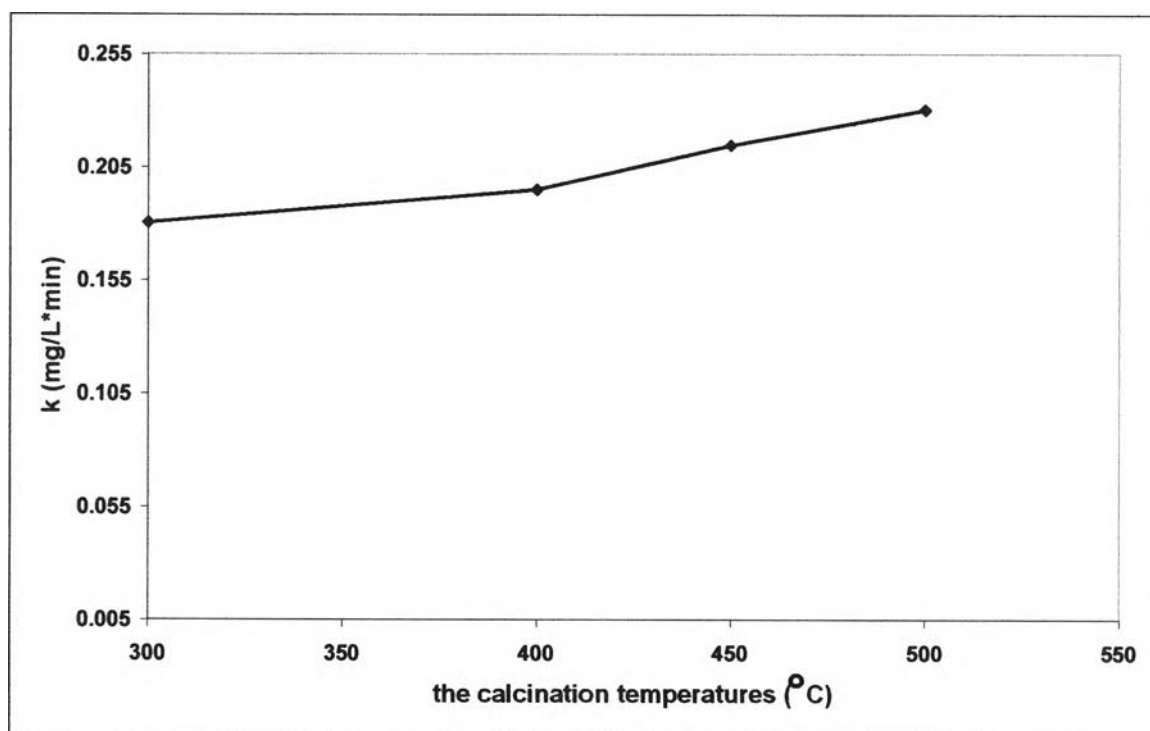
Figure 4.11 The plot of k VS the calcination temperatures

The results show that the difference of calcination temperatures is direct proportion to the different presence of the anatase structure. Table 4.14 demonstrated the variation time to complete the reaction. It is seen that at 500 °C the reaction is faster than the others which might be explained by the presence of the anatase phase at 500 °C. In contrast, the other reactions would slowly occur depending on the amount of anatase phase in TiO_2.

Table 4.14 The time to complete all of the reduction reactions at the variation of temperatures

Calcination temperatures (°C)	Time to complete the reaction (min)
300	139
400	128
450	116
500	109

For the summarization, it has been found that this phenomenon of the various temperatures affected mainly on the crystal structure. The anatase structure can be appeared at 400-500 °C. It is clearly seen that the crystalline size is the main important effect in this experiment. On the other side, the thickness does not play a role as a factor of the calcination temperatures. It is shown that from the SEM micrographs, at the higher temperatures the films would be uniformed more than at the low temperatures. From this point of view, when the temperature has been increasing, the size of the crystal tends to be decreased. So, the active surface area will be increased dependable on the size of the crystal. The more active surface area, the more kinetic coefficient (k) dedicates.

4.3 Effect of the coating cycles

The thickness of TiO_2 thin films is regulated by repeating the cycle from dipping to heat treatment. It can be performed by preparing the TiO_2 sol- solution in the mole ratio of titanium (IV) butoxide: ethanol: HCl: acetyl acetone equal to 1: 30: 0.5: 1, respectively. In this examination, a stainless steel plate played a role as a substrate was dipped, withdrawn and heated at 500 °C for 30 minutes with respect to 1, 2, 3, 4 and 5 times, respectively.

4.3.1 The physical properties

4.3.1.1 Adhesive test

The adhesive test (ASTM D3359-95a) was supplied by the adhesive tape (the scotch tape) to examine the stability, uniformity and adherence of the TiO_2 thin layers. Table 4.15 showed the results of the TiO_2 thin films prepared with different coating cycles were passed this test.

Table 4.15 The results which all conditions varied in the different coating cycles.

The number of coating cycles	Testing
1	passed
2	passed
3	passed
4	passed
5	passed

4.3.1.2 Corrosive test

From the results of this test, all of the different coating cycles were passed the test. This test was applied to find the film robustness and corrosive resistance under the acidic and basic conditions. The results were shown in Table 4.16.

Table 4.16 The results which all conditions varied in the different coating cycles

Acidic and Basic conditions	1 Cycle	2 Cycles	3 Cycles	4 Cycles	5 Cycles
1 M HNO$_3$	p	p	p	p	p
5 M HNO$_3$	p	p	p	p	p
10 M HNO$_3$	p	p	p	p	p
1 M NaOH	p	p	p	p	p
5 M NaOH	p	p	p	p	p
10 M NaOH	p	p	p	p	p

P = passed

4.3.2   Crystallization of TiO_2 thin films by XRD (X-ray diffraction)

Figure 4.12 showed the XRD patterns of TiO_2 thin films prepared with several coating times on stainless steel substrates. The intensity of 1-coating cycle gives the lowest intensity of anatase phase; definitely, its thickness is the thinnest. In this study, as the increasing of the number of coating cycles from 1-5 cycles, the amount of anatase tends to be increasing dependable upon the higher number of coating cycles. All the anatase peaks show at the angle of $25.28°$, $36.94°$, $37.8°$ and $38.58°$. With increasing the coating cycles, the anatase peaks become more intense. This indicates that high amount of crystallization of the anatase TiO_2 is resulted from several cycles of coating.

It is interesting to note that Fe in a stainless steel support reacted with O_2 and diffused from the air, forming an interlayer of iron oxide during an annealing treatment (Zhu et al., 2001). However, the diffusion of iron oxide did not change the electronic structure of the TiO_2 (Zhu et al., 2001). In order to banning the diffusion of Fe, the film thickness would be provided the multilayer. It is seen that the more proceeding layers, the more intensity of the anatase phase. Kajitvichyanukul et al., 2005 studied the effect of phase transformation of TiO_2 on the number of coating cycles. It was found that the raising of coating cycles up to 5, the rutile appeared when using the material support as the glass plate. Additionally, the phase transformation from the anatse to rutile might be increasing with extending of the coating cycles. In this work, the rutile did not occur at the 5-coating cycle using stainless steel plates. Perhaps, the effect of acetyl acetone may help to aggregate grains of TiO_2 and accelerate the formation of TiO_2 crystals in the films.
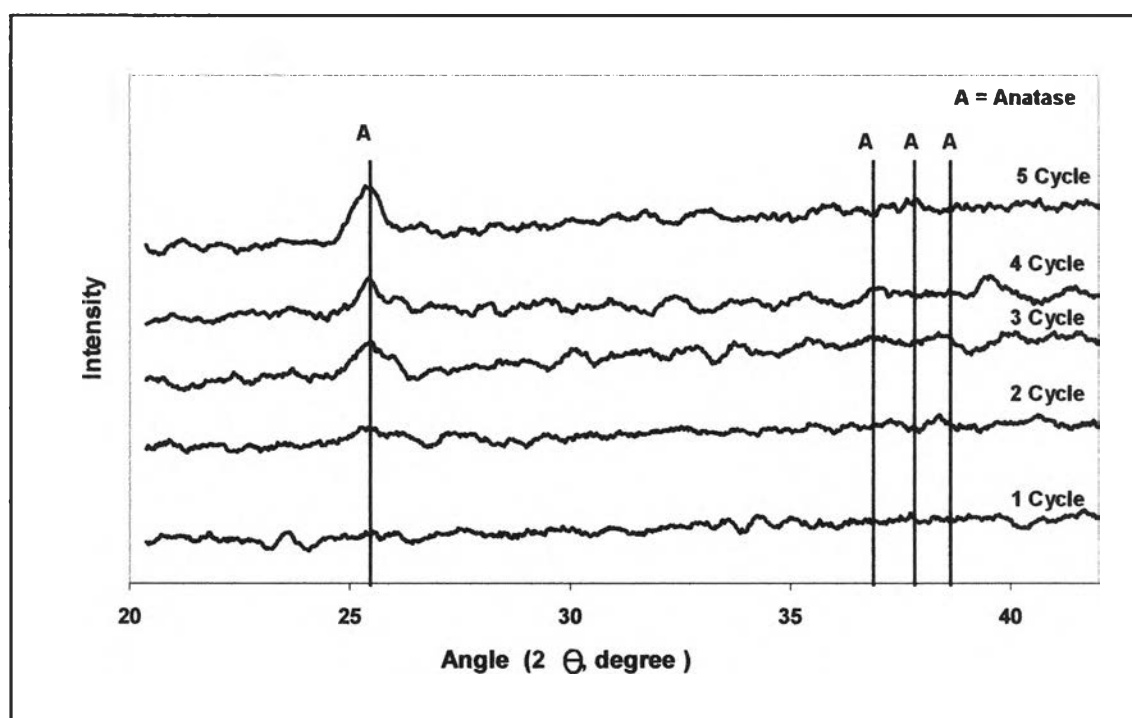
Figure 4.12   XRD patterns of TiO_2 thin films derived with different coating cycles

Table 4.17 Crystallite sizes of TiO_2 films prepared from different coating cycles

The number of coating cycles	Crystalline size (nm)
1	-
2	15.95
3	16.3
4	19.95
5	22.8

Table 4.17 manifested the crystallite size of the TiO_2 thin films prepared from the different coating cycles. It is ultimately seen that when the number of coating cycles have been increased, the crystalline anatase size would be slightly increased as the plot of the crystallite size versus the number of coating cycles shown in Figure 4.13. As seen in Figure 4.13, from the 3-coating cycles to the 5-coating cycles the trend tends to be

increased slightly. Before this entire trend, from the 1-coating cycle the film is too thin, so it cannot be calculated. This is to say that when the number of coating cycles increase, the crystal size of the anatase structure will be increased. So, the surface area will be slightly decreased due to its crystal size.
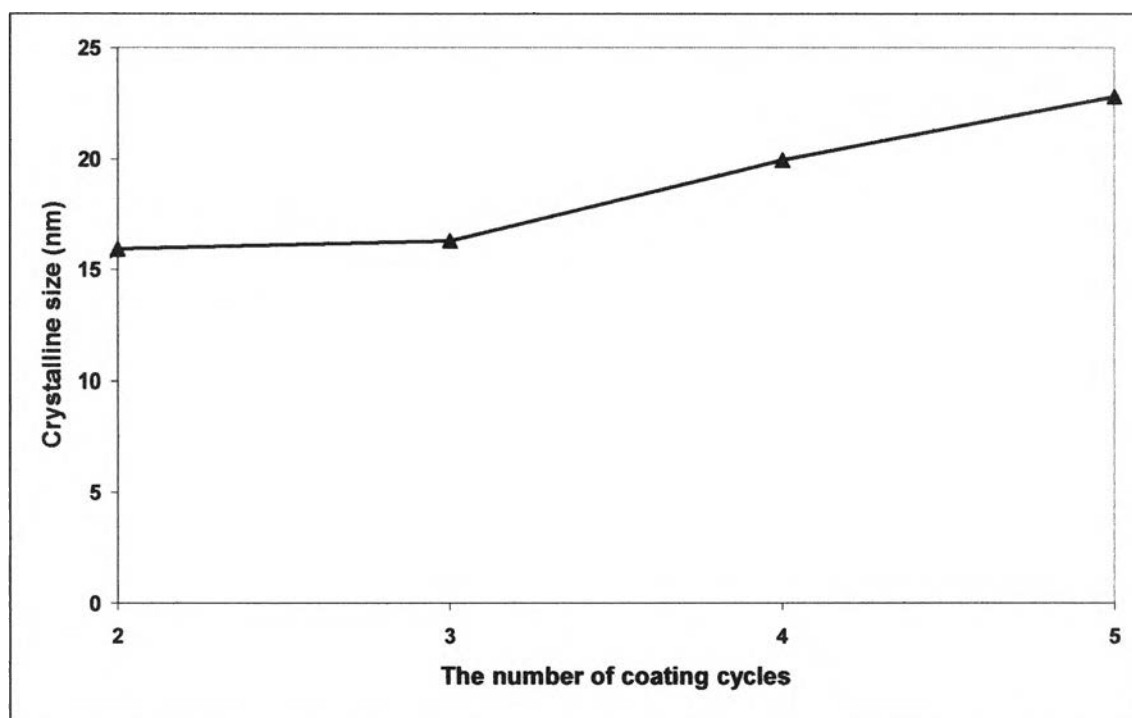

Figure 4.13   The plot of the crystallite size and the number of coating cycles

4.3.3   Thickness

The thickness is resulted when the number of coating cycles increase in terms of the multilayer. This makes this study especially interesting. Different TiO_2 thin layers corresponding to different thickness as indicated in Table 4.18. This table illustrated the thickness of the TiO_2 thin films prepared from the different coating cycles. It is worth to know that when the number of coating cycles increase, the thickness will also be increased significantly. Figure 4.14 demonstrated the trend of the thickness versus the number of coating cycles. The thin layer surface was rather irregular and this practically

independently of the film thickness (Lottiaux et al., 1989). It was slightly reduced on increasing thin layer thickness from 35 to 70 nm. Each layer was made of blocks around 40 nm in size and each block was made of smaller blocks (approximately ten times smaller) (Lottiaux et al., 1989). Figure 4.15 was the FE-SEM micrographs of TiO_2 thin films coated with various coating times from 3 to 5 coating cycles.

Table 4.18 The thickness of the TiO_2 films prepared from different coating cycles

The number of coating cycles	Thickness (nm)
1	33
2	70
3	91
4	130
5	165

Nevertheless, the higher thickness of TiO_2 thin films may give the worse efficiency of the photocatalytic reduction. When the TiO_2 thin films are thick, the excited electrons cannot rapidly go onto the surface. So, the electrons will recombine with a hole at the valence band that can be performed at the higher coating cycle number, the efficiency will be decreased as much as the multilayer thin films represent. The so-called of this situation is "*recombination*". As implied in the photocatalytic activities, there is only one condition which is optimum for the photocatalytic reduction of Cr (VI). From this important point, the more thickness provides, the more recombination occurs (Linsebigler et al., 1995; Liqiang et al., 2003; Shang et al., 2003).
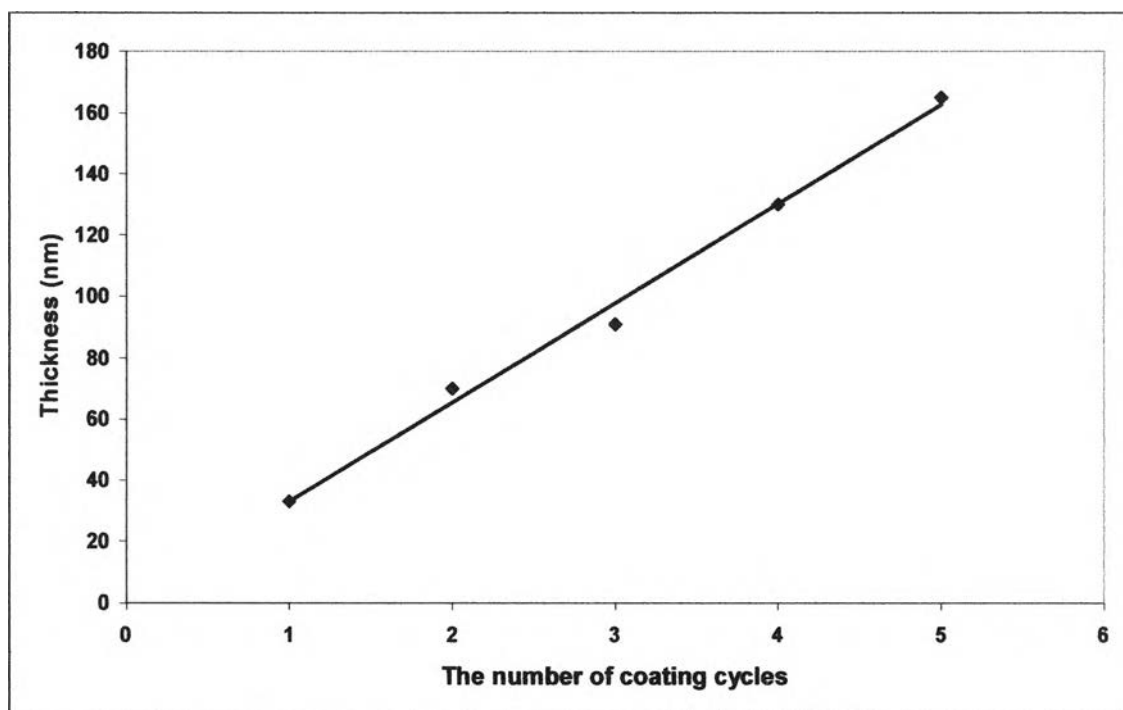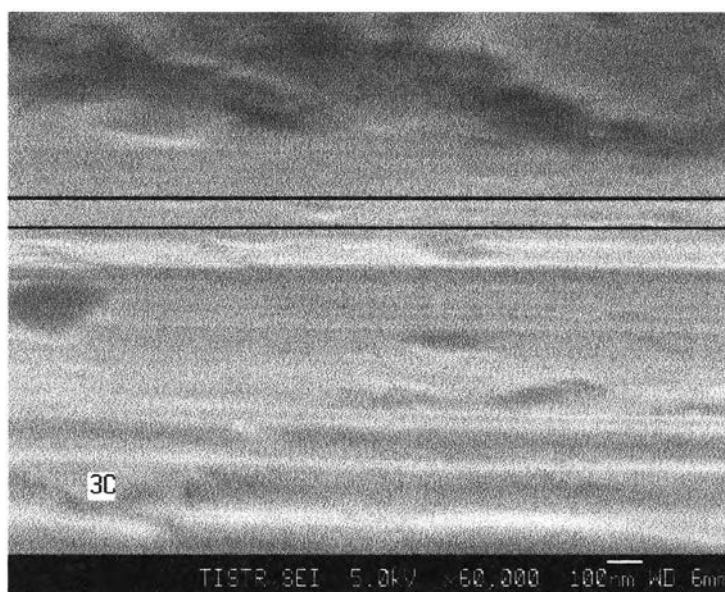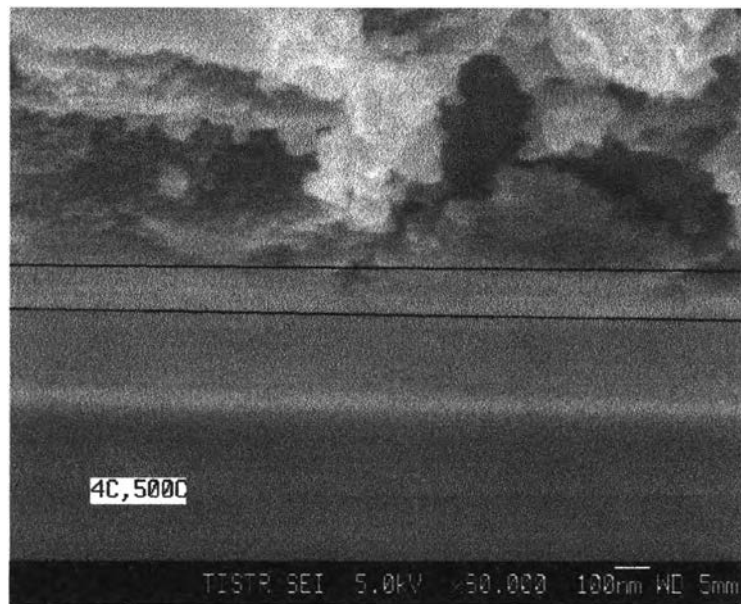
Figure 4.14 The plot of the thickness VS the number of coating cycles

60,000 magnifications

(a) TiO$_2$ thin films coated with 3-coating cycle

60,000 magnifications

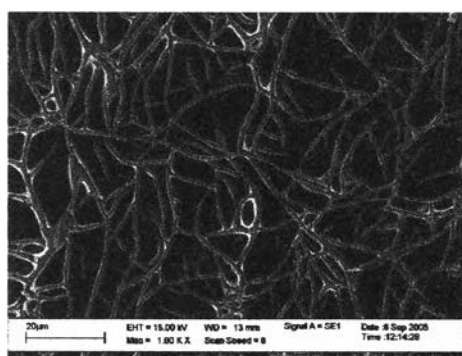(b) TiO$_2$ thin films coated with 4-coating cycle

60,000 magnifications
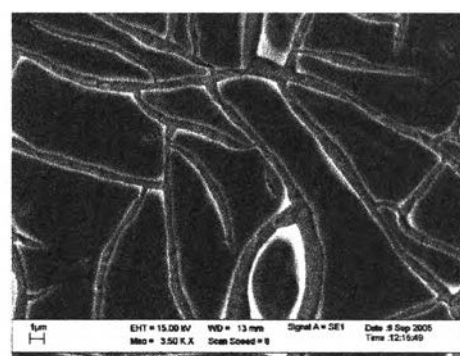
(c) TiO$_2$ thin films coated with 5-coating cycle

Figure 4.15 (a-c)   FE-SEM micrographs of TiO$_2$ thin films coated with
different coating cycles

4.3.4 The morphology of TiO₂ varied with the coating cycles

Figure 4.16 showed the SEM photographs of the surface of TiO₂ thin films prepared from 1-5 coating cycles and heat-treated at 500 °C for 30 minutes. It is observed that from 1 to 3 coating cycles the fractures tend to be decreased when the numbers of coating cycles increase. On the other side, from 4 to 5 coating cycles the cracks might be increased in which the numbers of coating cycles increase. This discrepancy gives an idea that at the lower coating cycles (smaller thickness), the films would be too thin and the thickness would also be smaller than at the larger coating cycles (higher thickness). However, at the higher coating cycles the cracks would be occurred, because the granular microstructure is sphere particles (Yu et al., 2000). The stability is also less than the 3-coating cycles. It seems apparently the 3-coating cycles gives the best reaction rate in the photocatalytic reduction.
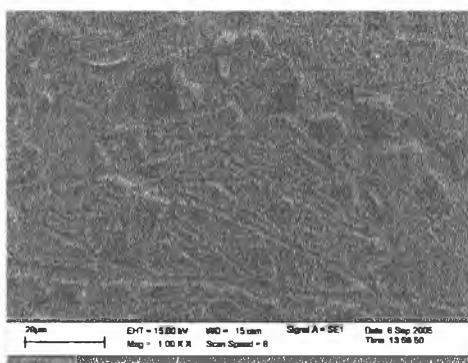

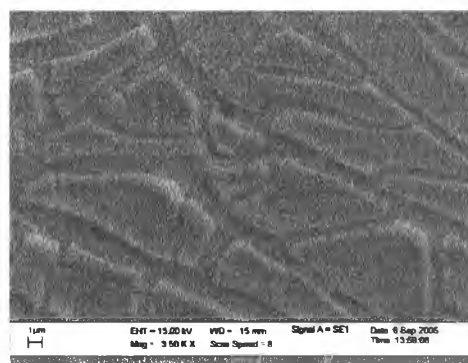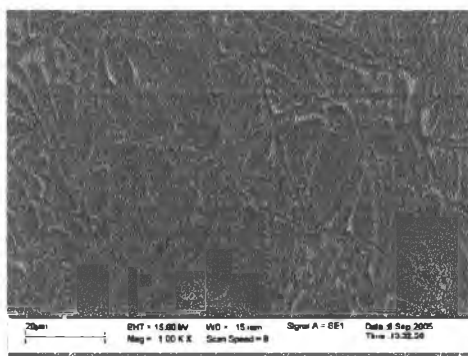1000x magnification   3500x magnification

(a) TiO₂ thin films coated with 1-coating cycle

1000x magnification   3500x magnification

(b)   TiO$_2$ thin films coated with 2-coating cycle
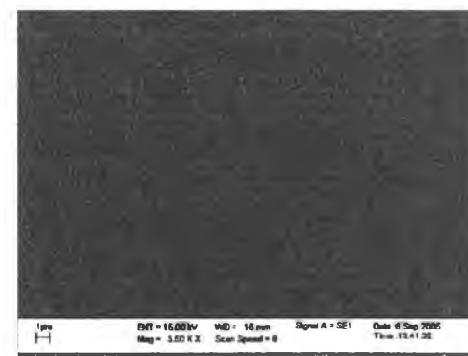

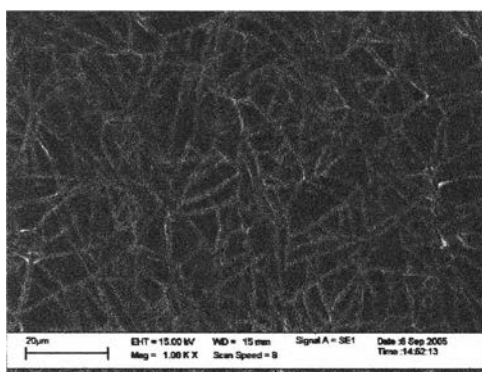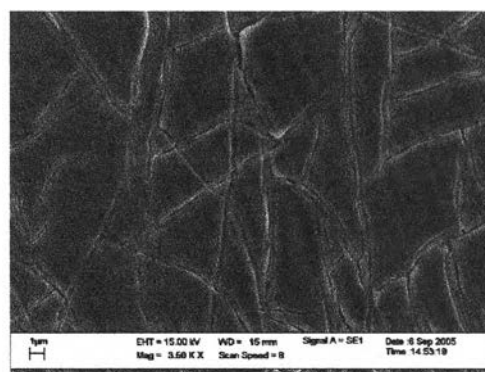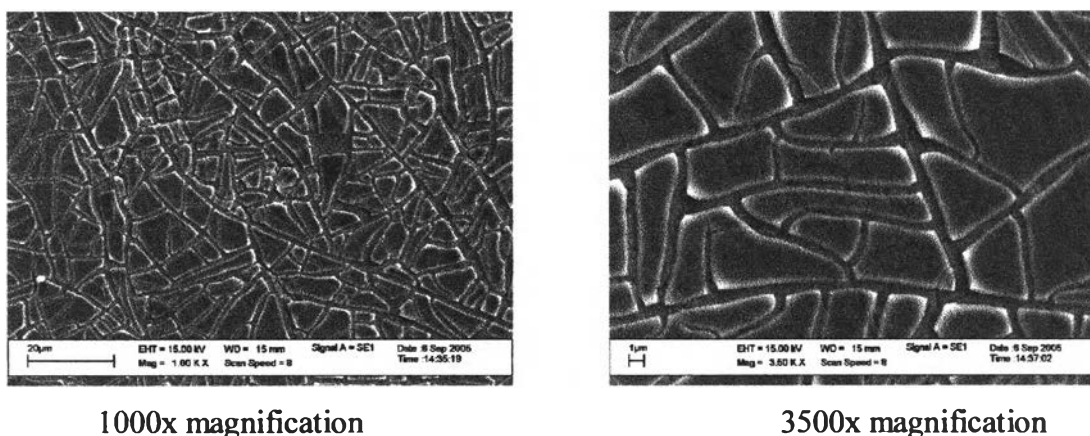1000x magnification   3500x magnification

(c)   TiO$_2$ thin films coated with 3-coating cycle

1000x magnification   3500x magnification

(d)   TiO$_2$ thin films coated with 4-coating cycle

| 1000x magnification | 3500x magnification |

(e) TiO$_2$ thin films coated with 5-coating cycle

Figure 4.16 (a-e)   SEM micrographs of TiO$_2$ thin films coated with different coating cycles from 1 to 5 coating cycles, respectively

4.3.5   Kinetic coefficient of the photocatalytic reduction

As the thin film samples in this study, the kinetic coefficient (k) is determined by varying the coating cycles. Figure 4.17 illustrated the reaction rate of all various coating cycles from 1 – 5 times. It is clearly seen that the best coating cycle number is 3-coating cycle. It makes the fastest reaction and spends very short time to complete the reaction. On the other hand, the worst coating cycle number is 5-coating cycle. Its reaction rate is the slowest. In addition to this phenomenon, the electrons in an electronically exited molecule (M*) can move down to the valence band molecule rapidly (M^0). It is so called in terms of a recombination (Oppenländer, 2003).

Actually, the raising of Cr (VI) removal efficiency may also relate to the expanding of the thickness (the number of coating cycles) of TiO$_2$. As shown in Figure 4.17, the reaction rate should be increasing from 1-coating cycle up to 3- coating cycle. Then the reaction rate might be decreasing from 4- coating cycle to 5-coating cycle. This situation can be explained that the recombination of TiO$_2$ occurs from 4-coating cycle up to 5-

coating cycle. It is due to the thickness of TiO$_2$ films with respect to the recombination occurs. From this case, it is explained that the thicker TiO$_2$ films can be produced the recombination. So, when the recombination occurs, the efficiency of the photocatalytic reduction may be decreased significantly that will also make the little kinetic coefficient value (k). Table 4.19 showed all of the kinetic coefficient values (k). And Figure 4.18 demonstrated the plot of k VS the number of coating cycles. Its trend can confirm the reason that is why the 3-coating cycle is the best condition and it made the highest k-value.
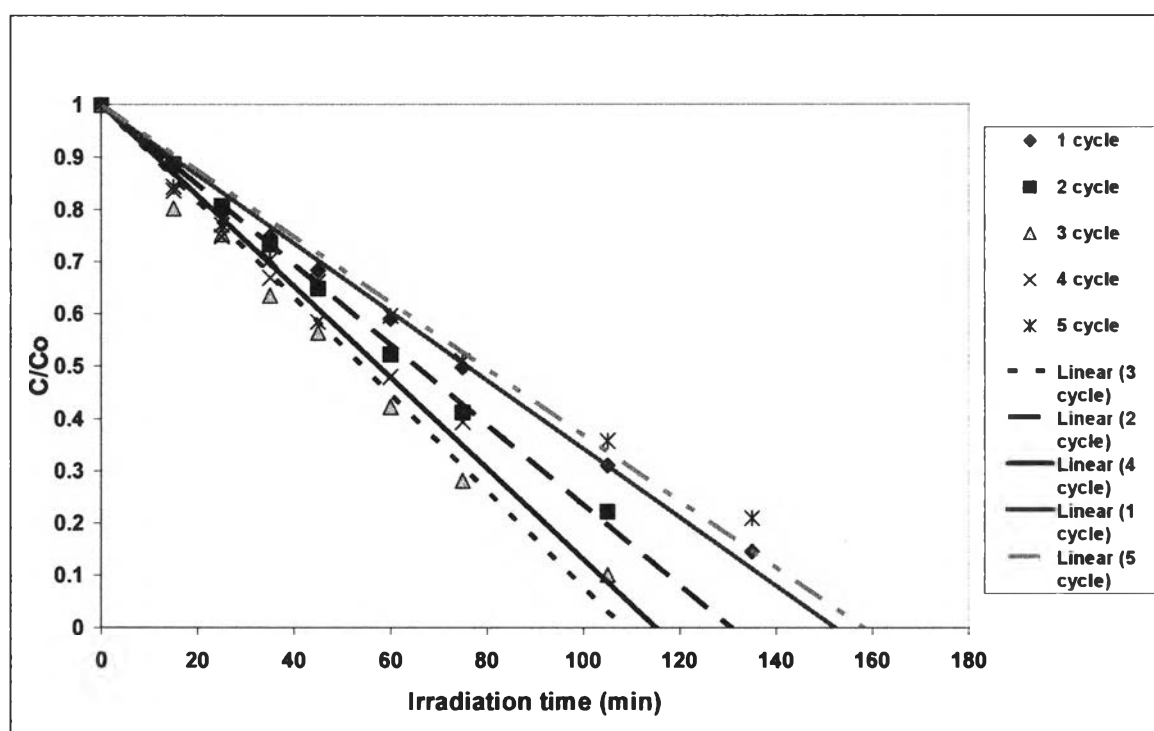

Figure 4.17   The photocatalytic reduction of Cr (VI) removal on the TiO$_2$

thin films prepared at the different coating cycles

Table 4.19 The kinetic coefficient values of the TiO_2 thin films
derived at the various coating cycles

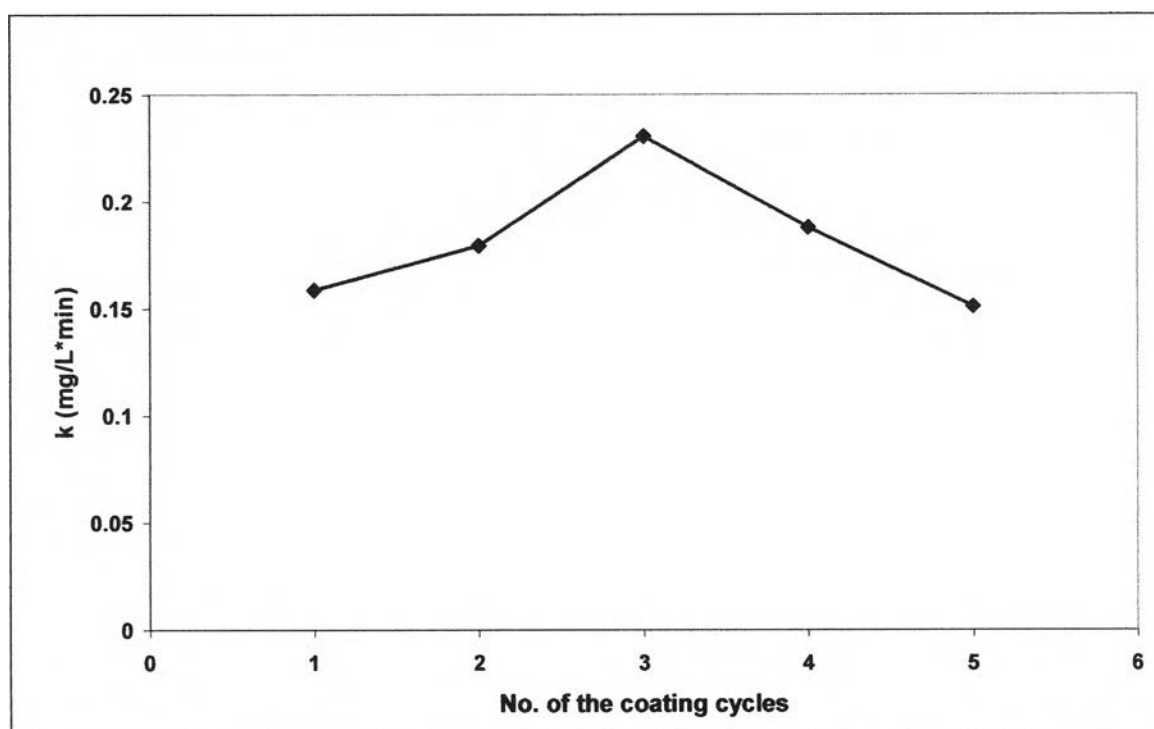| Coating cycles	Kinetic coefficient (k) (mg/L*min)	R^2
1	0.1588	0.9886
2	0.1796	0.9808
3	0.2306	0.9793
4	0.188	0.9498
5	0.151	0.958

Figure 4.18 The plot of k versus the number of coating cycles

The reduction reaction time of TiO_2 prepared with the different thickness (the coating cycles) were shown in Table 4.20. It is important to note that the 3-coating cycle

reaches an equilibrium faster than the others. The time of consumption in this process is 109 minutes. It is connected to the reason that is given earlier. It is likewise this case, the photocatalytic activity, based on the disappearance rate of malic acid, increased monotonically with the number of coatings (or film thickness) (Guillard et al., 2002).

Table 4.20 The time to complete all of the reduction reactions with the different coating cycles

Coating cycles	Time to complete the reaction (min)
1	152
2	130
3	109
4	115
5	159

In summary, all of the information in this experiment would give some factors which influence the efficiency of the number of coating cycles. Those factors are the thickness and the crystallite size. The thickness controls the amount of the anatase phase representing in each layer. The increasing of thickness may also give the higher amount of the anatase structure. Moreover, the crystalline size will affect the efficiency in the photocatalytic processes due to the surface area. When the increasing of the crystallite size represents, the surface area will be decreased. In contrast, the optimum condition of the coating cycles is the 3-coating cycles. In this case, the thickness more than the 3-coating cycles can affect the photocatalytic reduction with respect to the recombination may easily occur. As the information shown above, the kinetic coefficient value (k) can be seen the optimum circumstance as found at the 3-coating cycles. Moreover, the SEM micrographs would also imply the smoothest surface morphology at the 3-coating cycles. All information are connected to each other and conducted to the best photocatalytic process.

4.4 Effect of UV wavelengths

The variation of the reduction reaction rate as a function of the wavelength ensues the absorption spectrum of the catalyst, with a threshold corresponding to its band gap energy (Herrmann, 1999). Moreover, TiO_2 having $E_g = 3.20$ eV, this craves: $\lambda \leq 400$ nm, i.e., near UV wavelength (UV-A) (Herrmann, 1999). In this experiment, the best conditions of the previous work, which were TiO_2 thin films with adding acetyl acetone calcined at 500 °C with 3-coating cycles, were used to test the efficiency of the different wavelengths.

4.4.1 Kinetic coefficient of the photocatalytic reduction

Figure 4.19 showed the reaction rate of TiO_2 irradiated with different wavelengths. In this study, the appropriate wavelength is at 380 nm. Nevertheless, at 420 nm the reaction rate is the worst. At 254 nm, the reaction rate is quite good for removing Cr (VI) in the wastewater, but the TiO_2 irradiated at 380 nm is better than that. In general, the UV wavelength can be divided to 3 regions; UVA (320-400 nm), UVB (280-320 nm), and UVC (200-280 nm). According to these wavelengths, at 254 nm is a wavelength of which is the UVC (200-280 nm) (Phillips, 1983). The pollutants and the water constituents (dissolved organic and inorganic compounds) absorb the radiation in the UVC region (Phillips, 1983). However, at 380 nm represents a wavelength in the UVA region. This region contains the wavelength from 320-400 nm.

This is to say, the reaction with illumination at 380 nm occurs intensively corresponding to the band gap energy of TiO_2 (Eg = 3.20 eV) (Linsebigler et al., 1995; Fujishima et al., 1999; Litter, 1999). TiO_2 can adsorb the light in this wavelength mostly, so the electron-hole pairs can highly proceed in this wavelength. Thus, this circumstance will make the highest efficiency of photocatalytic reduction of Cr (VI).

Accordingly, at 254 nm TiO_2 can adsorb the light but it is not better than the light irradiation at 380 nm. The efficiency at 254 nm of photocatalysis in this test tends to be

less than the efficiency at 380 nm of photocatalysis. Thus, the kinetic coefficient at 254 nm would be less than the kinetic coefficient at 380 nm.

In contrast, at 420 nm is a wavelength in the visible. It has been suggested that this wavelength is broaden to accelerate the reduction reaction depending on the band gap of TiO_2. In the visible region, the energy can not exist to activate the electrons in the valence band (VB) to be the electrons in the conduction band (CB). So, the efficiency of this reaction with illumination at 420 nm is the least. The fewer electrons at the conduction band provide the less photocatalytic reduction efficiency that might give the lowest kinetic coefficient (k).

Figure 4.20 showed the plot of k VS the wavelengths. It has been seen that the k value in the UVA region (320-400 nm) is the best. After this region, the k value tends to be decreasing when the wavelength increases over 400 nm. Table 4.21 demonstrated the kinetic coefficient values (k) of the TiO_2 thin films using the different wavelengths.
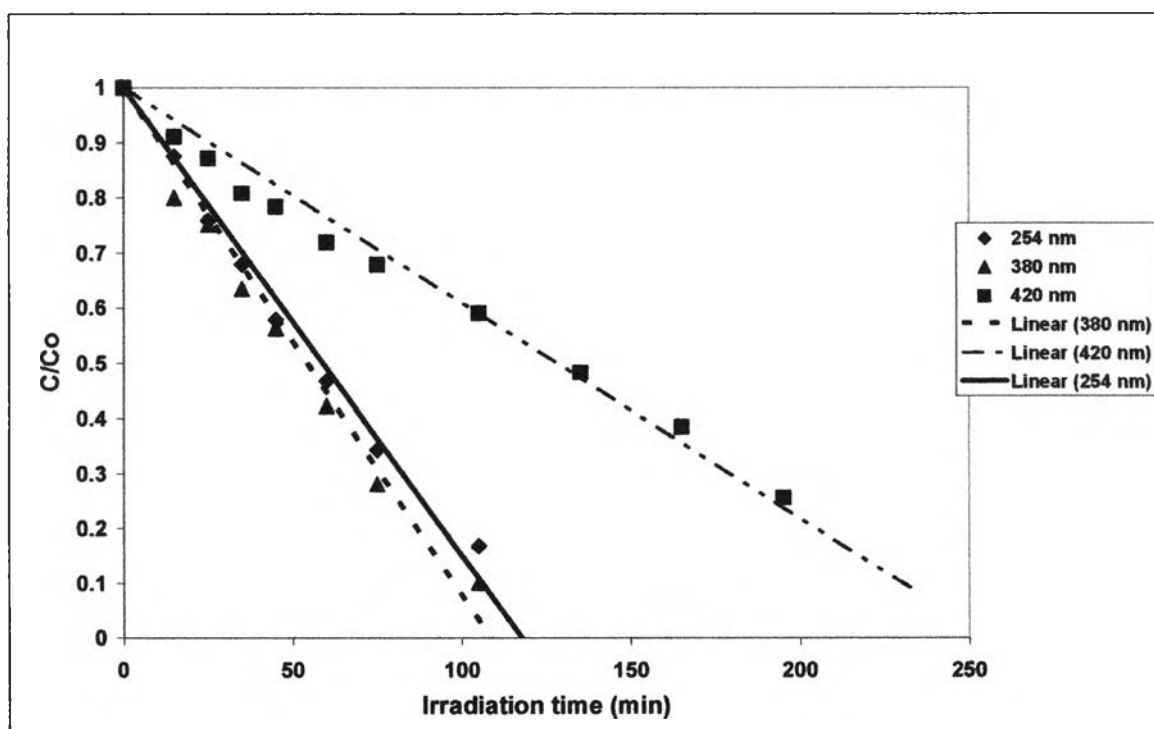

Figure 4.19   The photocatalytic reduction of Cr (VI) removal on the TiO_2 thin films irradiated with the different wavelength

Table 4.21   The kinetic coefficient values of the TiO$_2$ thin films
using the different wavelengths.

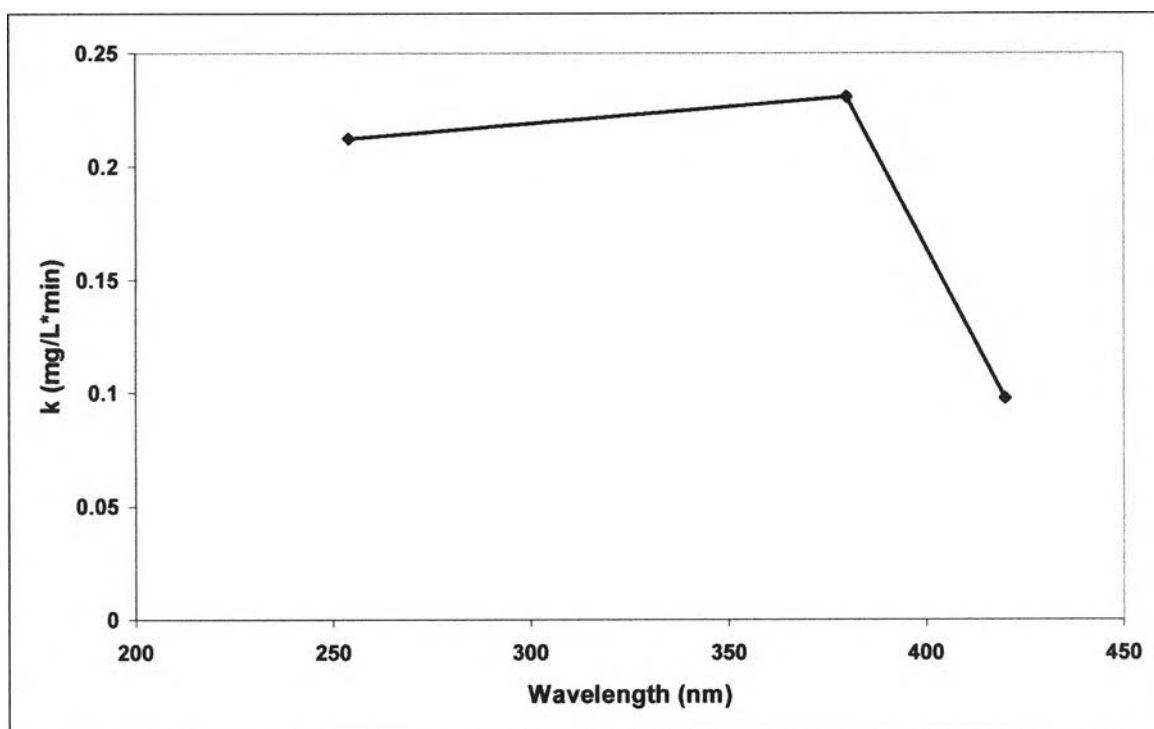| Wavelengths (nm)	Kinetic coefficient (k) (mg/L*min)	R^2
254	0.2123	0.9859
380	0.2306	0.9793
420	0.0977	0.9798

Figure 4.20   The plot of k versus the wavelengths

Table 4.22 illustrated the time to complete all of the reduction reactions with the different wavelengths. It is related to the photocatalytic activities that are mentioned earlier. At 380 nm, the reaction reaches the equilibrium faster than the others. On the other side, at 420 nm the reaction moves slower to reach the equilibrium. This may take more time to complete the reaction. However, at 254 nm the reaction tends to reach the equilibrium slower than the reaction irradiated at 380 nm.

Table 4.22 The time to complete all of the reduction reactions with the different wavelengths

Wavelength (nm)	Time to complete the reaction (min)
254	118
380	109
420	256